



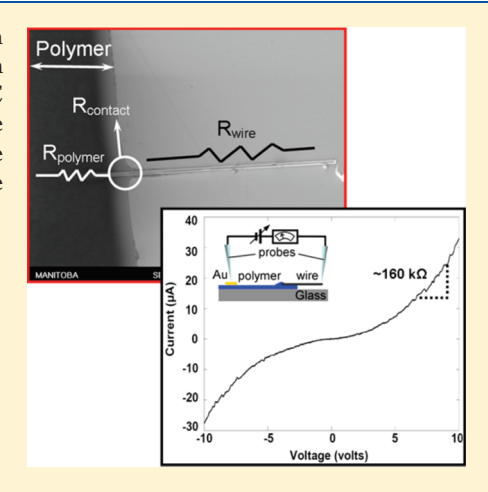
# Electrical Characterization of Si Microwires and of Si Microwire/Conducting Polymer Composite Junctions

Iman Yahyaie, <sup>†</sup> Kevin McEleney, <sup>‡</sup> Michael Walter, <sup>§</sup> Derek R. Oliver, <sup>†</sup> Douglas J. Thomson, <sup>†</sup> Michael S. Freund, <sup>\*,†,‡</sup> and Nathan S. Lewis <sup>\*,§</sup>

<sup>†</sup>Department of Electrical and Computer Engineering and <sup>‡</sup>Department of Chemistry, University of Manitoba, Winnipeg, MB, Canada <sup>§</sup>Division of Chemistry and Chemical Engineering, M/C 127-72, 210 Noyes Laboratory, California Institute of Technology, Pasadena, California 91125, United States

Supporting Information

**ABSTRACT:** The electrical (DC) behavior of single silicon microwires has been determined by the use of tungsten probes to make ohmic contact to the silicon microwires. The basic electrical properties of the microwires, such as their DC resistivity and the doping distribution along the length of the microwires, were investigated using this approach. The technique was also used to characterize the junction between silicon microwires and conducting polymers to assess the suitability of such contacts for use in a proposed artificial photosynthesis system.



**SECTION:** Energy Conversion and Storage

An artificial photosynthetic system, such as the one described by Gray, represents a promising conceptual approach to the production of fuels from sunlight.<sup>1</sup> Reducing this vision to practice will require the development of an integrated system that uses water and sunlight as inputs to generate hydrogen and oxygen as outputs.<sup>2,3</sup>

A functioning solar water-splitting device (Figure 1) would consist of three main components: a membrane-supported assembly that captures sunlight and, in turn, that efficiently creates separated electrons and holes which have sufficient chemical potential to drive the water-splitting reactions; a two-electron catalyst to facilitate reduction of protons to  $H_2$  at the cathode; and a four-electron catalyst for oxidation of water to  $O_2$  at the anode. The membrane will need to act as a physical barrier between the oxidation and reduction reactions and also must efficiently transport the electrons and protons that are generated at the catalyst sites.

The membrane-supported assembly, which in one implementation would include an array of doped silicon microwires supported in a conducting polymer film, will likely be a chemically complex structure that has critical features on the micrometer scale. Silicon microwire arrays are currently used in a wide range of applications from solar cells<sup>4–7</sup> to organic, liquid junction, and inorganic solid-state devices and offer an interesting platform to develop a photocathode for  $H_2$  production from water in the presence of suitable electrocatalysts.

A variety of different electrical parameters, such as the Si microwire resistivity as well as the doping distribution and the total series resistances in the microwire/conducting polymer system, will have to be optimized to produce acceptable overall device performance. The nature of the electrical junctions between doped silicon microwires and different candidate conducting polymers will thus be an important factor in the proper function of the final water-splitting device (Figure 1). The goal of this work was to develop methods to enable facile characterization of the electrical properties of the Si microwires as well as characterization of the junctions between these microwires and the conducting polymer component of the membrane that will be required to obtain a complete, functional solar fuel generation system.

The Si microwires investigated in this work were grown using the vapor—liquid—solid chemical vapor deposition (CVD) process. <sup>9,12,13</sup> The single-crystalline Si microwires were 60—120  $\mu$ m in length and ~1.5—2.0  $\mu$ m in diameter. The Si microwires were doped to two different levels of boron,  $10^{17}$ — $10^{18}$  (highly doped) and  $10^{15}$ — $10^{16}$  cm<sup>-3</sup> (low-doped), by introduction of BCl<sub>3</sub>(g) during wire growth.

Received: January 28, 2011 Accepted: February 25, 2011 Published: March 04, 2011

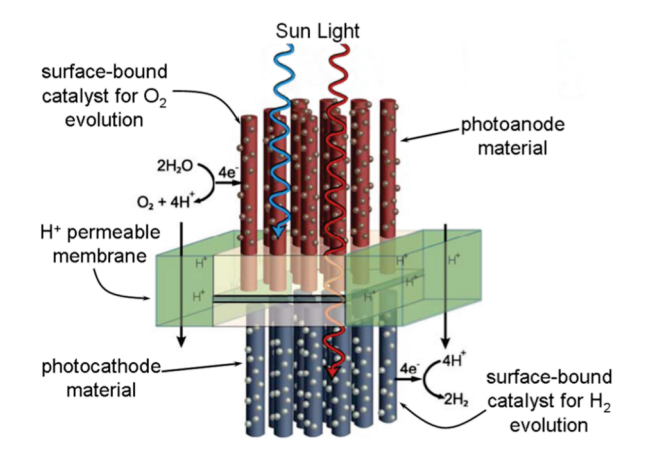


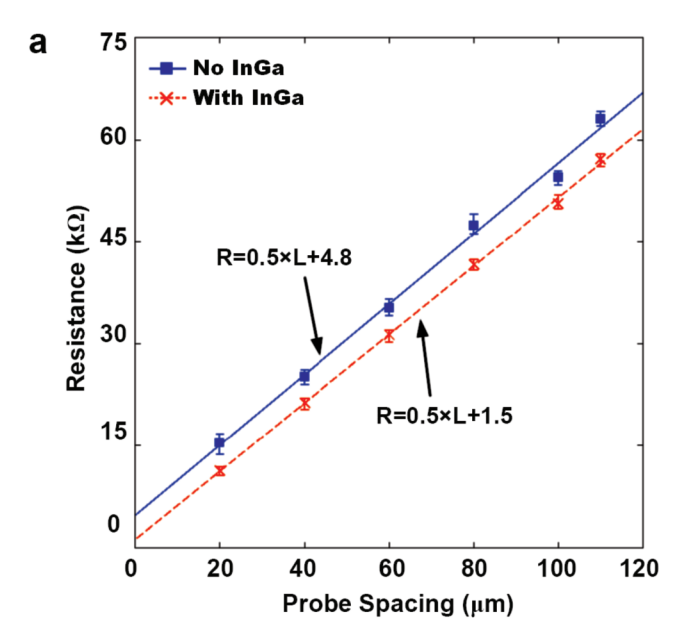
**Figure 1.** Schematic diagram of the proposed artificial photosynthesis system; reprinted with permission from ref 3.

In previous work, ohmic contacts suitable for electrical measurements have been made to individual Si microwires by the thermal evaporation of contact metals. <sup>14–16</sup> Although this method provides a high-yield procedure for contact formation, the lithographic, high-temperature process is only applicable to a certain range of microwire diameters and is not compatible with microwire/polymer combinations.

In this work, the electrical properties of single silicon microwires and of Si microwire/polymer junctions have been characterized using a simple, reproducible method of contact formation. Specifically, tungsten (W) probes were used to make direct contacts to HF-etched Si microwires that had been deposited on a glass substrate (see Supporting Information). The tungsten probes allowed for mechanical manipulation of the microwires and also enabled the formation of electrical contacts to the individual wires. These probes were also used to make good electrical contacts to silicon by use of the conventional, electrically conductive, fluid indium/gallium (In/Ga) metal eutectic as an interfacial metallic phase. The Current voltage (I-V) measurements were then performed at various probe separations along the microwires.

These measurements had three main goals, (1) to show that the measurement was unaffected by variation in the positions of the probes along the microwires, (2) to determine the value of contact resistance between the probes and the microwires, and (3) to investigate the uniformity of the doping concentration along the length of the microwires.

Figure 2 depicts the resistance versus probe separation data obtained for the highly doped and low-doped Si microwires, respectively. Each data point includes seven independent measurements in which the probe was completely disconnected from the microwire before the contact for the next measurement was made. These measurements therefore demonstrate that reliable and reproducible contacts to individual microwires were obtained. The resistance per unit length ( $\sim 0.5 \text{ k}\Omega \cdot \mu\text{m}^{-1}$  for the highly doped and  $\sim$ 14.2 k $\Omega \cdot \mu \text{m}^{-1}$  for low-doped microwires) remained constant for all of the measurements, with or without In/Ga as a contact method. This behavior verified that, other than a decrease in the value of the contact resistance, the nature of the contacts was unaffected by the presence or absence of In/ Ga. The contact resistance was calculated by performing a linear fit to the resistance versus probe separation data, in conjunction with evaluation of the intercept of such a plot (Figure 2). The



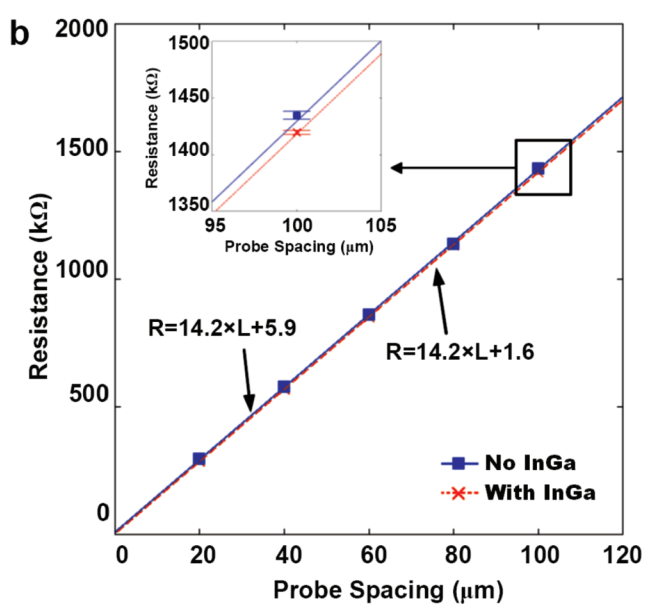
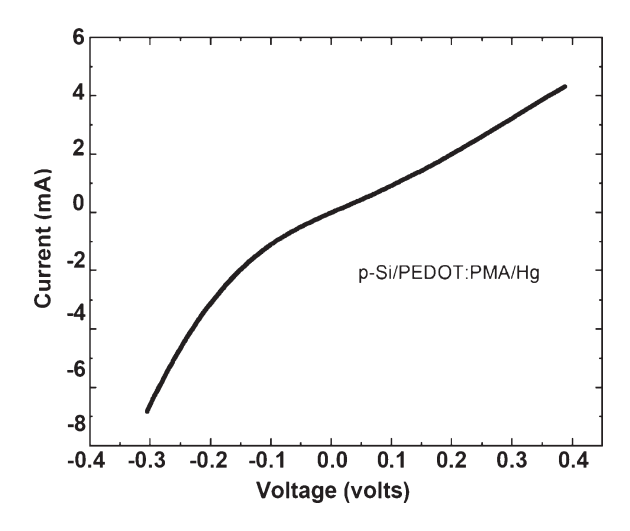


Figure 2. Contact resistance measurements for  $\sim$ 1.5  $\mu$ m (a) highly doped and (b) low-doped silicon microwires. Seven independent measurements were carried out for each selected point across the length of the microwire both with and without In/Ga (14 measurements in total at each point).

calculated contact resistance values from both types of microwires were in reasonable mutual agreement. Although the calculations showed that the contact resistance was a negligible contribution to the total measured resistance, the contact resistance was subtracted prior to calculating the resistivity of the microwires and, in turn, prior to the estimation of the doping concentration of the microwires.

The doping concentration of the highly doped microwires was estimated to be  $10^{17}-10^{18}~{\rm cm}^{-3}$ , which is within the expected range based on the conditions used to grow the Si wires of interest. No fluctuation in the resistances was observed between different regions of the microwires; therefore, the p-type dopant concentration appeared to be uniform at the length scales



**Figure 3.** PEDOT/PMA/planar p-Si junction and corresponding I-V curve. PEDOT/PMA was contacted with a Hg droplet. The p-Si wafer was etched in NH<sub>4</sub>F immediately prior to casting the PEDOT/PMA film. Slightly nonlinear behavior was observed for this junction.

considered. An analogous set of data indicated that the doping concentration of the low-doped microwires was  $10^{15}-10^{16}~{\rm cm}^{-3}$ .

The mechanism of contact formation between the W probes and the Si microwires is different than that of many conventional methods for producing ohmic contacts  $^{14-16}$  because the tungsten probes were applied directly to the Si microwire, with no high-temperature treatment or lithography required. One explanation for the observed electrical behavior of the W/Si wire contacts is the effect of local pressure at the point of contact. The resistivity of silicon is a function of pressure, as reported previously.  $^{19,20}$  Additionally, an abrupt transition, from a Schottky to an ohmic contact, was reported when a mechanical pressure of  $\sim \! 112000 \; \rm kg \cdot cm^{-2}$ , that is,  $\sim \! 11 \; \rm mN \cdot \mu m^{-2}$ , was applied to planar Si samples.  $^{21}$ 

The force exerted on the microwires by the tungsten probes was  ${\sim}12~{\rm mN}\cdot\mu{\rm m}^{-2}$  (see Supporting Information). Additionally, a lower pressure than that reported for planar Si might be required to induce a transition in silicon microwires because the reported pressure on planar silicon $^{21}$  was exerted through an interfacial Al layer. Furthermore, the amount of pressure required to induce a phase transition in silicon  $^{19}$  is a function of the Si doping density, and this factor may account for the difference in observed contact resistances between highly doped and low-doped Si microwires observed herein.

To investigate the behavior of the electrical junction between the polymers and silicon microwires, solutions of two candidate conducting polymers, polyethylenedioxythiophene/phosphomolybdic acid (PEDOT/PMA)<sup>22</sup> and polyehtylenedioxythiophene/polystyrene sulfonate/Nafion (PEDOT/PSS/Nafion)<sup>23</sup> with 12 wt % PEDOT/PSS, were prepared according to established procedures (see Supporting Information). The polymers were then coated onto planar silicon substrates that had the same doping concentrations as the Si microwires. Oxidatively doped polyacetylene has been shown to form ohmic contacts to p-Si.<sup>24</sup> However, the conducting polymers PEDOT/PMA and PED-OT/PSS/Nafion coated on both low-doped and highly doped silicon substrates exhibited slightly nonlinear I-V behavior (Figure 3). Although the silicon wafers were etched immediately prior to casting the films, it was anticipated that a thin layer of

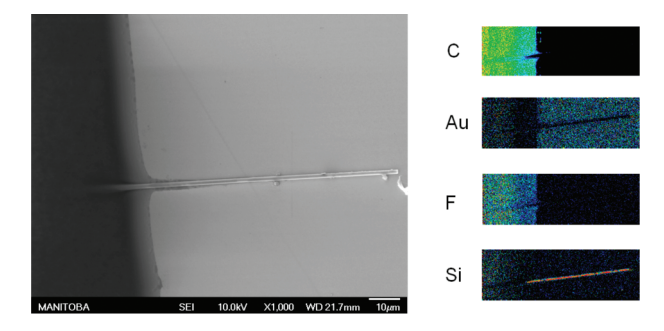


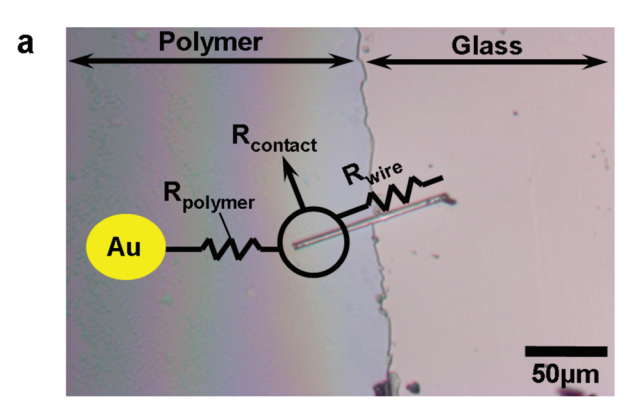
**Figure 4.** SEM image of a microwire embedded into a PEDOT/PSS/Nafion drop-cast film at the polymer/gold border (left) and Auger elemental analysis (right). The Auger image shows the localization of the polymer (C and F) on the right side of the image as well as the microwire (Si) extending from the polymer.

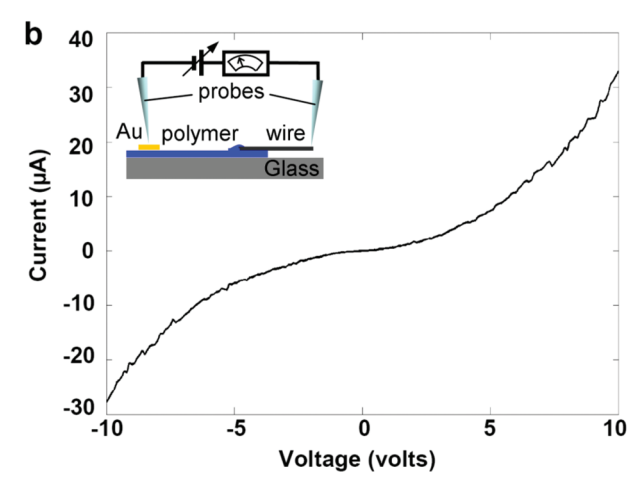
native oxide almost immediately formed on the surface, potentially through oxidation by PMA. Nonlinearity in the I-V behavior of such a junction at low voltages is likely due to tunneling through such an oxide layer. Such nonlinear behavior has been the subject of investigation in the literature. Hence, the total resistance values for the system were measured at higher bias voltages, where such nonlinear behavior was not dominant and the I-V profile appeared purely resistive.

To investigate the behavior of silicon microwire/conducting polymer junctions, conducting polymer solutions were spin-coated onto a glass substrate, half of which was masked using Parafilm. After removal of the mask, the films were determined to be between 150 and 200 nm thick. Ohmic contacts to the conducting polymer films were then formed by sputtering a gold pad directly onto the polymer.

Following removal of the Parafilm mask, the microwires were deposited onto the exposed glass substrate. Using tungsten probes, single microwires were aligned at the border between the glass substrate and conducting polymer to make electrical contact. Scanning electron microscopy (SEM) and Auger electron spectroscopy (AES) imaging indicated an intimate contact between the polymer and microwire, as well as a sharp border between the polymer and substrate (Figure 4). Unlike the samples used for electrical characterization, a drop-cast film of PEDOT/PSS/Nafion was prepared on a gold-coated slide to alleviate charging issues for the SEM and AES analysis. AES imaging indicated that both carbon and fluorine were localized in the polymer, with a decrease in intensity observed where the microwire entered the polymer. Examining the image for silicon, the microwire was clearly present both inside of the polymer as well as over the gold substrate. The gold image also showed the void region where the microwire covered the gold

Using the tungsten probes, the microwires aligned in the polymer films were then covered with a small amount of polymer to enhance the electrical contact between the polymer and the microwires. This configuration is more representative of the final envisioned device structure, in which part of the microwire would be embedded inside of the conducting polymer membrane (Figures 1 and 4). The three main junctions present in the final measurement system are therefore the sputtered gold/polymer junction, the tungsten probe/microwire junction, and the microwire/polymer junction in between (Figure 5a). The sputtered gold/polymer junction exhibited well-defined ohmic characteristics (see Supporting Information). The tungsten probe/microwire





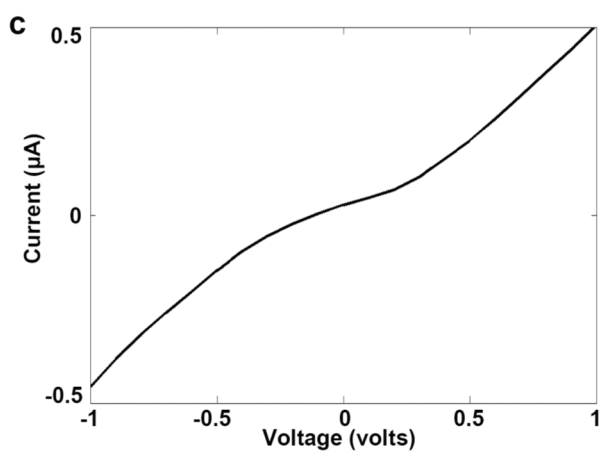


**Figure 5.** (a) A 100 μm long highly doped microwire with a diameter of  $\sim$ 1.5 μm aligned at the polymer/glass border and the measured I-V profile for different ranges of applied bias voltages, (b) -10 to +10 V and (c) -1 V +1 V. The total series resistance of the system is  $\sim$ 160 k $\Omega$ .

junction was also investigated in the first set of measurements. Its contribution to the total resistance (in the form of contact resistance) was negligible compared to the contribution of the other resistances. The experiments were performed by recording the current passing through the system for different applied voltages, having one tungsten probe in contact with the microwire while the other one was placed on the gold contact (see Supporting Information). An I-V profile for a highly doped microwire aligned at the PEDOT/PSS/Nafion/glass border is shown in Figure 5b,c. The total series resistance including  $R_{\rm polymer}$ ,  $R_{\rm cr}$  and  $R_{\rm wire}$  from this measurement

Table 1. Measured Resistances in M $\Omega$   $(\pm 1\%)^a$ 

| $R_{\mathrm{wire}}$ | $R_{\mathrm{PMA}}$ | $R_{\mathrm{PSS/Naf.}}$ | $R_{c(\mathrm{PMA})}$ | $R_{\rm c(PSS/Naf.)}$ |
|---------------------|--------------------|-------------------------|-----------------------|-----------------------|
| 1.42                | ~1.32              | ~0.008                  | 9.75                  | 1.40                  |
| 0.05                | ~1.32              | ~0.008                  | 0.30                  | 0.10                  |

 $^a$  The microwire length and diameter are 100 and 1.5  $\mu m$ , respectively.  $R_{\rm PMA}$  and  $R_{\rm c(PMA)}$  are the resistance of the PEDOT/PMA film and the calculated resistance of the junction between low-doped (1st row) and highly doped (2nd row) microwires and the films.  $R_{\rm PSS/Naf.}$  and  $R_{\rm c(PSS/Naf.)}$  represent the same parameters for PEDOT/PSS/Nafion films.

was  $\sim$ 160 k $\Omega$ . The microwire/polymer contact resistance ( $R_c$ ) was then calculated from the expression

$$R_{\text{tot}} = R_{\text{polymer}} + R_{\text{wire}} + R_{\text{c}}$$

where  $R_{\rm tot}$  is the total resistance of the microwire/polymer system,  $R_{\rm polymer}$  is the resistance of the conducting polymer, calculated from four-point probe measurements, and  $R_{\rm wire}$  is the microwire resistance. The contact resistances involved in the system (tungsten probe/microwire contact resistance) were all significantly smaller than these resistances. Table 1 summarizes all of the measured resistances for both highly doped and low-doped Si microwires.

To estimate the performance of these microwire/polymer combinations in the proposed artificial photosynthesis device, the maximum reported terrestrial cell and submodule efficiency as measured under the global air mass (AM) 1.5 spectrum (1000  $\rm W\cdot m^{-2})$  at 25 °C was taken to be 42.7 mA·cm<sup>-2</sup> for a monocrystalline silicon solar cell. Considering this value as the maximum short-circuit photogenerated current density from an array of 100  $\mu m$  long microwires,  $^{6,27,29}$  the absorption of all of the photons falling on the membrane area would result in a current of  $\sim\!20.9$  nA in each microwire.

Assuming a maximum voltage drop of ~10 mV along the microwire/membrane junction and the same amount of current (20.9 nA) flowing through the junction to the polymer film, the total resistance in the microwire/polymer system should be less than 480 k $\Omega$ . The resistance of a PEDOT/PMA junction with highly doped microwires is therefore greater than, but very close to, the critical value, whereas the PEDOT/PSS/Nafion junction with highly doped Si microwires definitely meets the minimum conductance requirements. As mentioned earlier, these values were calculated at large bias voltages ( $\pm 10 \text{ V}$ ). At bias voltages close to the actual expected working conditions ( $\pm 10 \text{ mV}$ ), higher resistances were observed, indicating the importance of the microwire surface treatment (e.g., native oxide removal etc.) on the electrical properties of the Si/polymer junctions. In contrast, the junction between highly doped Si microwires PEDOT/PMA exhibited significant resistance at these current levels. Although the PEDOT/PSS/Nafion junction with highly doped Si microwires was less resistive, improvements in IR losses at these low current levels were required to meet the minimum requirements for a final device.

In summary, a novel electrical contact approach was used to characterize the (DC) electrical properties of two important sections of a proposed artificial photosynthesis device. The method employed tungsten probes (with or without In/Ga) to make good electrical contacts to silicon microwires. The advantage of this method is that the contact could be formed only by applying force to the probe—microwire junction, alleviating the need for a high-temperature treatment. The local pressure in the immediate contact area of the silicon microwire resulted in a local

phase transition and resulted in the observed, reproducible, ohmic contact. The measured resistances were in agreement with the expected doping levels for the microwires. <sup>14,18</sup> The electrical junction between single silicon microwires and two conducting polymer films was also investigated. The results of these measurements have helped to define the required electrical properties for the individual microwires and for the candidate conducting polymers to be used in a working artificial photosynthesis device to produce fuels directly from sunlight.

## ASSOCIATED CONTENT

Supporting Information. Metallic catalyst removal procedure, conductive polymer film preparation, microwire/polymer junction formation, quantifying the applied mechanical force on the single silicon microwires, and additional figures. This material is available free of charge via the Internet at http://pubs.acs.org.

### AUTHOR INFORMATION

#### **Corresponding Author**

\*E-mail: michael\_freund@umanitoba.ca. Tel: +1~204~474-8772~ (M.S.F.); E-mail: nslewis@caltech.edu. Tel: +1~626~395-6335~ (N.S.L.).

#### ACKNOWLEDGMENT

Financial support from the following is gratefully acknowledged: The Technology International Collaboration Fund of Manitoba Innovation Energy and Mines, the Natural Sciences and Engineering Research Council (NSERC) of Canada, the Canada Foundation for Innovation (CFI), the Manitoba Research and Innovation Fund, and the University of Manitoba. The work reported made use of the Manitoba Institute for Materials. This work was also supported by the NSF through a Center for Chemical Innovation, by the Stanford Global Trust and Energy Program, and by Toyota and made use of the Molecular Materials Research Center of the Beckman Institute at Caltech and the Kavli Nanoscience Institute at Caltech. This research was undertaken, in part, thanks to funding from the Canada Research Chairs Program.

#### ■ REFERENCES

- (1) Gray, H. B. Powering the Planet with Solar Fuel. *Nat. Chem.* **2009**, *1*, *7*.
- (2) Walter, M. G.; Warren, E. L.; McKone, J. R.; Boettcher, S. W.; Mi, Q.; Santori, E. A.; Lewis, N. S. Solar Water Splitting Cells. *Chem. Rev.* **2010**, *110*, 6446–6473.
- (3) CCI Powering the Planet: An NSF Center for Chemical Innovation; California Institute of Technology, http://ccisolar.caltech.edu (Retrieved Nov. 2010).
- (4) Tsakalakos, L.; Balch, J.; Fronheiser, J.; Shih, M. Y.; Leboeuf, S. F.; Pietrzykowski, M.; Codella, P. J.; Korevaar, B. A.; Sulima, O. V.; Rand, J.; Davulura, A.; Rapol, U. Strong Broadband Optical Absorption in Silicon Nanowire Films. *J. Nanophoton.* **2007**, *1*, 1355/2–1355/10.
- (5) Peng, K.; Xu, Y.; Wu, Y.; Yan, Y.; Lee, S. T.; Zhu, J. Aligned Single-Crystalline Si Nanowire Arrays for Photovoltaic Applications. *Small* **2005**, *1*, 1062–1067.
- (6) Hu, L.; Chen, G. Analysis of Optical Absorption in Silicon Nanowire Arrays for Photovoltaic Applications. *Nano Lett.* **2007**, 7, 3249–3252.

- (7) Tian, B.; Zheng, X.; Kempa, T. J.; Fang, Y.; Yu, N.; Yu, G.; Huang, J.; Lieber, C. M. Coaxial Silicon Nanowires as Solar Cells and Nanoelectronic Power Sources. *Nat. Lett.* **2007**, *449*, 885–889.
- (8) Huynh, W. U.; Dittmer, J. J.; Alivisatos, A. P. Hybrid Nanorod-Polymer Solar Cells. *Science* **2002**, *295*, 2425–2427.
- (9) Maiolo, J. R. I.; Kayes, B. M.; Filler, M. A.; Putnam, M. C.; Kelzenberg, M. D.; Brunschwig, B. S.; Atwater, H. A.; Lewis, N. S. High Aspect Ratio Silicon Wire Array Photoelectrochemical Cells. *J. Am. Chem. Soc.* 2007, 129, 12346–12347.
- (10) Goodey, A. P.; Eichfeld, S. M.; Lew, K. K.; Redwing, J. M.; Mallouk, T. E. Silicon Nanowire Array Photoelectrochemical Cells. *J. Am. Chem. Soc.* **2007**, *129*, 12344–12345.
- (11) Boettcher, S. W.; Warren, E. L.; Putnam, M. G.; Santori, E. A.; Turner-Evans, D. B.; Kelzenberg, M. D.; Walter, M. G.; McKone, J. R.; Brunschwig, B. S.; Atwater, H. A.; Lewis, N. S. Photoelectrochemical Hydrogen Evolution Using Si Microwire Arrays. *J. Am. Chem. Soc.* **2011**, 133, 1216–1219.
- (12) Kayes, B. M.; Filler, M. A.; Putnam, M. C.; Kelzenberg, M. D.; Lewis, N. S.; Atwater, H. A. Growth of Vertically Aligned Si Wire Arrays over Large Areas (>1 cm<sup>2</sup>) with Au and Cu Catalysts. *Appl. Phys. Lett.* **2007**, *91*, 103110–110113.
- (13) Wagner, R. S.; Ellis, W. C. Vapor—Liquid—Solid Mechanism of Single Crystal Growth. *Appl. Phys. Lett.* **1964**, *4*, 89–90.
- (14) Kelzenberg, M. D.; Turner-Evans, D. B.; Kayes, B. M.; Filler, M. A.; Putnam, M. C.; Lewis, N. S.; Atwater, H. A. Photovoltaic Measurements in Single-Nanowire Silicon Solar Cells. *Nano Lett.* **2008**, *8*, 710–714.
- (15) Koren, E.; Rosenwaks, Y.; Allen, J. E.; Hemesath, E. R.; Lauhon, L. J. Nonuniform Doping Distribution along Silicon Nanowires Measured by Kelvin Probe Force Microscopy and Scanning Photocurrent Microscopy. *Appl. Phys. Lett.* **2009**, *95*, 092105–092107.
- (16) Allen, J. E.; Perea, D. E.; Hemesath, E. R.; Lauhon, L. J. Nonuniform Nanowire Doping Profiles Revealed by Quantitative Scanning Photocurrent Microscopy. *Adv. Mater.* **2009**, *21*, 3067–3072.
- (17) Shapley, J. D. L.; Barrow, D. A. Novel Patterning Method for the Electrochemical Production of Etched Silicon. *Thin Solid Films* **2001**, 388, 134–137.
- (18) Putnam, M. C.; Turner-Evans, D. B.; Kelzenberg, M. D.; Boettcher, S. W.; Lewis, N. S.; Atwater, H. A. 10  $\mu$ m Minority-Carrier Diffusion Lengths in Si Wires Synthesized by Cu-Catalyzed Vapor—Liquid—Solid Growth. *Appl. Phys. Lett.* **2009**, 95, 163116–163118.
- (19) Paul, W.; Pearson, G. L. Pressure Dependence of the Resistivity of Silicon. *Phys. Rev.* **1955**, *98*, 1755–1757.
- (20) Bridgman, P. W. The Effect of Pressure on the Electrical Resistance of Certain Semi-Conductors. *Proc. Am. Acad. Arts Sci.* **1951**, *79*, 127–148.
- (21) Bradby, J. E.; Williams, J. S. In Situ Electrical Characterization of Phase Transformations in Si During Indentation. *Phys. Rev. B* **2003**, 67, 085205–085209.
- (22) McFarlane, S. L.; Deore, B. A.; Svenda, N; Freund, M. S. A One-Step, Organic-Solvent Processable Synthesis of PEDOT Thin Films via In Situ Metastable Chemical Polymerization. *Macromolecules* **2010**, 43, 10241–10245.
- (23) McFarlane, S. L.; Day, B. A.; McEleney, K.; Freund, M. S.; Lewis, N. S. Designing Electronic/Ionic Conducting Membranes for Artificial Photosynthesis. *Energy Environ. Sci.* **2011**, 10.1039/C0EE00384K.
- (24) Sailor, M. J.; Klavetter, F. L.; Grubbs, R. H.; Lewis, N. S. Electronic Properties of Junctions between Silicon and Organic Conducting Polymers. *Nature* **1990**, *346*, 155–157.
- (25) Card, H. C.; Rhoderick, E. H. Studies of Tunnel MOS Diodes I. Interface Effects in Silicon Schottky Diodes. *J. Phys. D: Appl. Phys.* **1971**, *4*, 1589–1601.
- (26) Lo, S.-H.; Buchanan, D. A.; Taur, Y.; Wang, W. Quantum-Mechanical Modeling of Electron Tunneling Current from the Inversion Layer of Ultra-Thin-Oxide nMOSFET's. *IEEE Electron Device Lett.* 1997, 18, 209–211.
- (27) Green, M. A.; Emery, K.; Hishikawa, Y.; Warta, W. Solar Cell Efficiency Tables (Version 36). *Prog. Photovoltaic Res. Appl.* **2010**, *18*, 346–352.

- (28) Zhao, J.; Wang, A.; Green, M. A.; Ferrazza, F. 19.8% Efficient "Honeycomb" Textured Multicrystalline and 24.4% Monocrystalline Silicon Solar Cells. *Appl. Phys. Lett.* **1998**, *73*, 1991–1993.
- (29) Kayes, B. M.; Atwater, H. A.; Lewis, N. S. Comparison of the Device Physics Principles of Planar and Radial p—n Junction Nanorod Solar Cells. *J. Appl. Phys.* **2005**, *97*, 114302–114311.